

Integrated Multiphysics Modeling in Materials and Manufacturing Processes

J. H. Hattel

Abstract – Today, multiphysics modelling of single process steps as well as modelling of entire process sequences and the subsequent in-service conditions are areas which increasingly support optimization of manufactured parts. In the present paper two different examples of modelling manufacturing processes from the viewpoint of combined materials and process modelling are presented: i) Integrated modelling of spray forming and ii) Integrated multiphysics modelling of friction stir welding. The third example describes integrated modelling applied to a failure analysis of a premature rupture of a stellite weld on a P91 valve used in a powerplant. For all three examples, the focus is put on modelling results rather than describing the models in detail. Comparison with experimental work is given in all examples for model validation as well as relevant references to the original work. **Copyright © 2010 Praise Worthy Prize S.r.l. - All rights reserved.**

Keywords: *Integrated Modeling, Multiphysics, Spray Forming, Friction Stir Welding, Failure Analysis*

I. Introduction

In the field of manufacturing engineering it has become more and more evident that computer simulation is a must in the search for optimised products and structures. Today, complex thermal manufacturing processes such as casting and welding are often addressed with multiphysics models involving both Computational Fluid Dynamics (CFD) and Computational Solid Mechanics (CSM) as well as thermodynamic and kinetic models, see e.g. [1]-[6]. Recently, multiphysics modelling of welding has also been combined with optimization methods to achieve desired properties of the weld; e.g. Mishra et al. [7] make an optimization of the weld geometry with multiphysics modelling in combination with genetic optimization algorithms.

In addition to this, the integration of multiprocess steps and materials modelling has emerged as a new growing field which attracts some attention in literature, although, the amount of articles dealing specifically with the subject is still relatively limited. Crumbach et al. [8] make a through process modelling of aluminium sheet production following the microstructural evolution during the production steps involving casting, heat treatment and forming processes. Also Bellini et al. [9] analyse the heat treatment of cast parts. Kermanpur et al. [10] simulate the various stages of gas turbine disc manufacture to track defects throughout the entire process chain of melting, homogenisation heat treatment, cogging, forging, final heat treatment and machining. Gandin et al. [11] make an integrated model of casting,

solidification and heat treatment in order to predict the final yield stress of an Al-Cu cast alloy. Myhr et al. [12] presents a numerical model for microstructure and strength evolution in Al-Mg-Si alloys during ageing, welding and post heat treatment and Lundbäck et al. [13] simulate the sequence of Tig-welding and post weld heat treatment of an Inconel plate.

Recently, examples of mapping the results to a subsequent load analysis during service have emerged, e.g. Robin et al. [14] model phase distribution and residual stresses in spotwelding and maps the results to a subsequent crash calculation and Thorborg et al. [15] model the process sequence of welding a stellite 6 layer on a P91 valve followed by machining, heat treatment and in-service conditions in a power plant. For the heat treatment and in-service stages, the microstructural evolution due to diffusion in the satellite/P91 is taken into account also.

In the following, three different examples of describing and analysing different manufacturing processes from the viewpoint of integrated or multiphysics modelling of materials and processes will be presented, see Fig. 1. For each of the examples focus will be on a short introduction and presenting some essential results. The models will only be explained very briefly since the scope of the present paper is to give an overview of interesting research results rather than going into modelling details. For more specific information, proper references to the original work will be given for each of the presented examples. The three examples are the following (with references to the original work):

1. Integrated multiphysics modelling of spray forming [18]-[21], [26]-[29].
2. Integrated multiphysics modelling of friction stir welding [6], [33]-[35], [39]-[41].
3. Integrated multiphysics modelling for a failure analysis of a stellite weld on a P91 valve [15], [48].

The two first examples deal with modelling of individual processes, whereas the last example presents a case-story which has been analysed by integrated modelling, where an entire sequence of processes and subsequent service has to be taken into consideration.

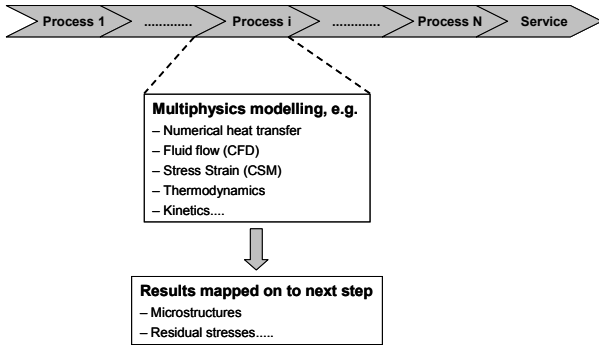


Fig. 1. Integrated modelling of consecutive process steps and service

II. Integrated Modelling of Spray Forming

The basic principle of the spray forming process is that molten metal is atomized in an inert or reactive atmosphere to give a spray of liquid particles. The particles are then collected onto a substrate situated below the point of atomization.

In the spray forming process, it is possible to spray form in different geometries such as tubes, billets or strips. The most common geometry is a cylindrical billet. This is produced either horizontally or vertically. In order to account for the growth of the billet, the substrate is moved continuously to keep a constant distance between the atomizer and the substrate. The spray forming process has been continuously modelled and described in literature. The models are often divided into two parts namely: atomisation and deposition. A major part of the models for atomisation are based on the idea that the continuous phase (gas) affects the properties of the dispersed phase (liquid melt) but not vice versa [16]-[17]. However, in a real system the droplets, which are represented by their size distribution do interact with each other via the gas and therefore a model that is able to reflect that, is desirable. This is accounted for in the model by Hattel and Pryds [18]-[19] which is based on a heat balance between the droplets and the surrounding gas by assuming a 1-D Eulerian frame, i.e. fixed finite control volumes along the centreline of the spray cone, assuming that the injected gas is only slightly expanded along the radial direction, see Fig. 2.

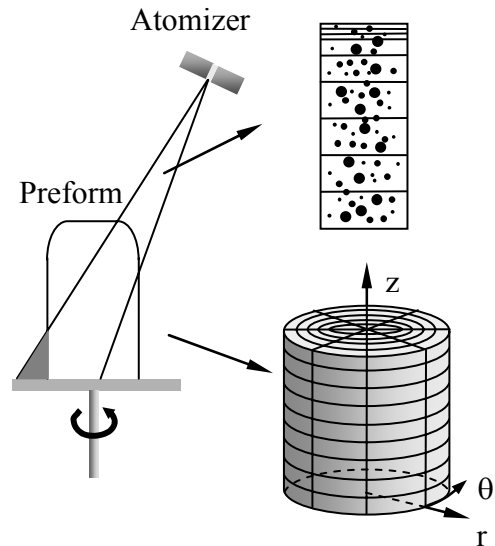


Fig. 2. Integrated model of the spray forming process consisting of a 1-D model of the atomization in the spray cone and a 3-D model of the deposition process. From Hattel and Pryds [40]

The interaction between the enveloping gas and an array of droplets given by the droplet distribution is coupled and calculated numerically. This enables a dynamic calculation of the gas temperature, thus avoiding the need for knowing it a priori. The model has been validated thoroughly against experiments [19]-[20]. A special validation study focused on relating the SDAS, the droplet diameter and the cooling rate both experimentally and numerically. Since it is very cumbersome directly to measure the cooling rate of atomizing droplets, a somewhat indirect approach for the experimental determination was taken. The SDAS was measured for different particle sizes of 100Cr steel and the relationship was found to follow an expression of the form:

$$\lambda_2 = B_1 d^m \quad (1)$$

where $B_1 = 0.64 \mu\text{m}^{1-m}$ and $m = 0.16$. Moreover, the relationship between SDAS and the cooling rate was measured for a casting of the same material in a wedge formed mould, resulting in a relationship of the form:

$$\lambda_2 = B_2 \dot{T}^{-n} \quad (2)$$

where $B_2 = 54.38 \text{ K}^n \text{ s}^{-n}$ is a preconstant depending on the kinetic terms of the system and $n = 0.33$ is the exponent of the cooling rate. Of course the cooling rate obtained in a wedge mould is considerably lower than that of atomising droplets, however, if it is assumed that the validity of Eq. (2) can be extrapolated to the higher cooling rate regime of rapid solidification, a combination of the equations (1) and (2) result in the following expression:

$$\dot{T} = B_3 d^{-m/n} \quad (3)$$

where the constants are found to be $B_3 = 3.54 \times 10^{-7} \text{ K s}^{-1} \text{ mm}^{m/n}$ and $m/n = 1.939$ respectively.

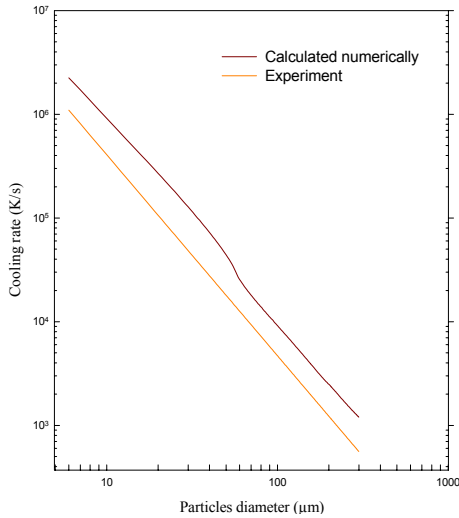


Fig. 3. Comparison between the experimentally based Eq. (3) and atomisation model for the cooling rate as a function of particle diameter. From Pryds, Hattel and Thorborg [31]

In Fig. 3, a comparison between the cooling rate as a function of particle diameter is given for the experimentally based Eq. (3) and the numerical atomisation model. The numerical calculations were conducted for argon gas and heterogeneous nucleation.

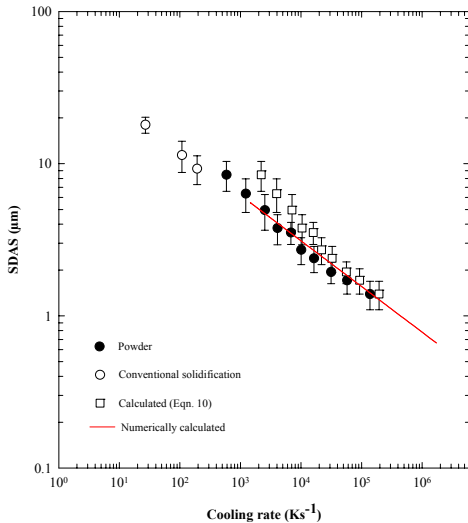


Fig. 4. SDAS as a function of the cooling rate for four different cases. Material: 100 Cr steel. From Pryds, Hattel and Thorborg [31]

A reasonably good agreement is found.

Fig. 4 shows the SDAS as a function of the cooling rate for four different cases: The Black circles denote the experimentally obtained values for the powder as given

by Eq. (2). The white circles denote the results from conventional solidification (at low cooling rates) in the wedge mould and the squares denote the results as obtained from the widely used simple relationship for the cooling rate of a single droplet cooled by a gas via a heat transfer coefficient of h , i.e.:

$$\dot{T} = \frac{6h(T_{melt} - T_{gas})}{\rho c_p^{liq} d} \quad (4)$$

Note, that Eq. (4) does not account for the spray being composed of multiple droplet sizes interacting with each other through the gas as a result of thermal coupling. As seen from Fig. 4, the numerical atomisation model predicts very well the experimentally found results for the SDAS as a function of the cooling rate.

An important feature of the atomisation model is that it takes thermal coupling into account, i.e. not only the gas temperature affects the thermal state of the droplets but also vice versa. A special study focusing on this thermal coupling was carried out by Hattel and Pryds [21].

Regarding the deposition, the models proposed in literature can be divided into two principally different approaches, i.e. purely geometrical models e.g. [22]-[23] and models, which take both the thermal and the geometrical effects into consideration, e.g. [24]-[25].

As an example of the latter, a 3-D cylindrical Finite Volume based model was developed by Hattel and Pryds for the thermal analysis of the growing deposit, e.g. Gaussian [26] or billet shape [27]-[28]. The model includes continuation of solidification after droplet impact as well. The model has been linked to the aforementioned atomisation model through a thorough coupling procedure. This involved among other two special features: a) Introduction of local droplet distributions along the radius of the spray cone enabling averaging of the enthalpy of impacting droplets as function of position on the surface and b) the implementation of a very detailed and general shadow algorithm not only involving backward face culling but being able to deal with all types of arbitrary geometries. This way, a unique integrated model of the spray forming process was established, taking into account both atomization and deposition in a coupled manner. The model has been used for predicting the evolution of the shape and thermal state of a spray formed billet as well as compared with experimental observations, Fig.6.

One of the important process parameters for controlling the quality of the spray formed billet in the industry is the surface solid fraction. This is very much dependent on the energy contained in the droplets dependent at the surface of the preform, i.e. the temperature and size of the droplets. Moreover, the droplet size distribution as well as the temperature of the droplets are dependent on the ratio between the gas flow and the melt flow and on the gas velocity. Hence, a way to control the

surface solid fraction during the process, is to control the ratio between the flow rate of the gas and the melt known as the Gas to Metal Ratio (GMR). Thus, the integrated model by Hattel and Pryds has been used in combination with experimental observations in order to establish a first suggestion for the influence of the GMR on the surface state in spray forming [29], i.e.:

$$T_{surface} = \frac{a}{\left(1 + \left(\frac{GMR}{x_0}\right)^b\right)} \quad (5)$$

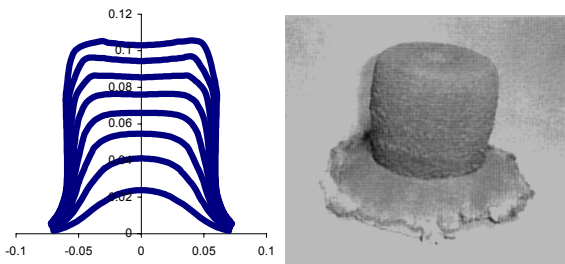


Fig. 5. Left: Prediction of billet shape of 100Cr6. Right: Experimentally obtained billet shape of 100Cr6 From Hattel et al.³⁹

Where a, b and x_0 are constants depending on the process parameters. a is a temperature [K] and x_0 corresponds to a reference value of the GMR. b is a dimensionless exponent.

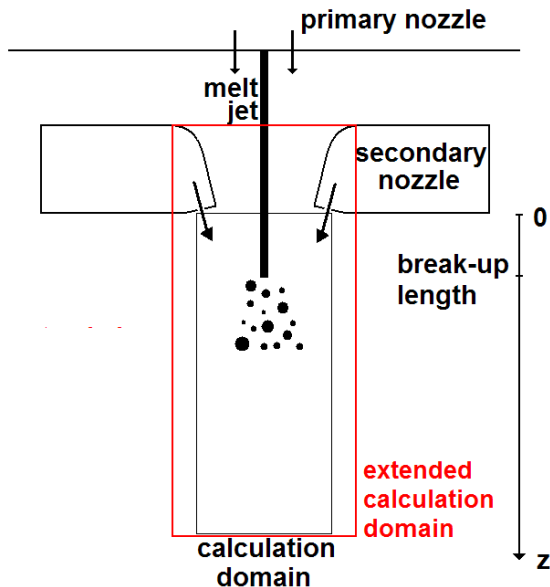


Fig. 6. Calculation for 3D calculation of coupled gas and droplet flow during spray forming. From Gjessing et al. [30]

Recently, the integrated model presented above had its flow model during flight improved by using a full 3D solution of the coupled flow problem of the interacting droplets and gas, implemented in the free software

OPENFOAM, see Gjessing et al. [30]. The calculation domain is shown in Fig. 6.

Special attention was paid to modeling the effect of both primary and secondary break-up of the droplets, Fig. 7.

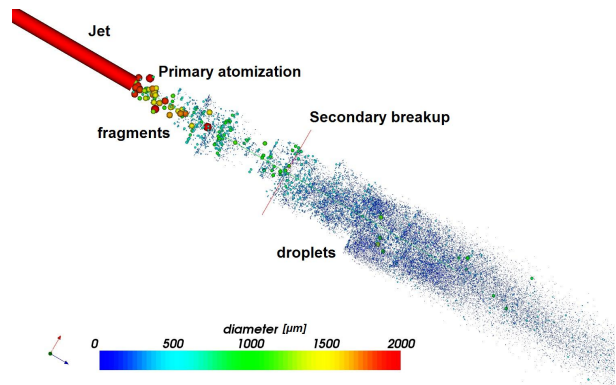


Fig. 7. Calculation for 3D calculation of coupled gas and droplet flow during spray forming. From Gjessing et al. [30]

III. Integrated Multiphysics Modeling of Friction Stir Welding

Friction stir welding (FSW) is a relatively new and complex solid state welding process in which the temperatures during the process reach a level close to the melting point as a result of both friction and plastic dissipation. In combination with a highly complex material flow initiated by the rotating tool, a joining of the two materials is achieved as for other welding processes.

Modelling FSW is a very challenging task. As indicated above it involves material flow, heat generation, large plastic deformations, strains and stresses all of which take place alongside and coupled with microstructural changes. This makes the modelling of FSW highly complex and interdisciplinary. This is also reflected in the modelling literature of FSW, which in essence could be divided into three different groups: i) Thermal models of FSW, e.g. [31]-[35] ii) Computational Fluid Dynamics (CFD) models of FSW, e.g. [36]-[41] and iii) Computational Solid Mechanics (CSM) models of FSW, e.g. [42]-[45].

III.1. Thermal Models of FSW

In the thermal models of FSW the basis of the model is a moving heat source emulating the heat input from the rotating tool. During this movement the temperatures in the calculation mesh are determined. The knowledge about the size and distribution of the heat source must be known somehow a priori to the calculation. Typically this information will come from experiments or from more advanced computational solid mechanics models. The obvious advantage of pure thermal models is that they use very little CPU-time. On the other hand they

also rely solely on the quality of the input description of the heat source since no material flow or thermomechanics is taken into account.

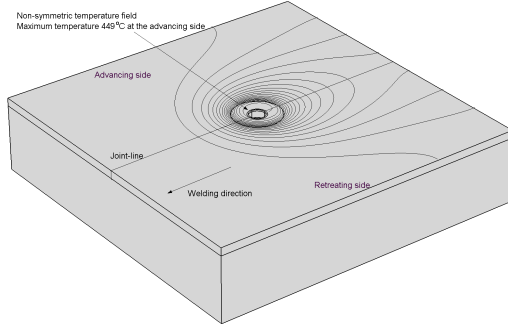


Fig. 8. Isotherms on top surface of two plates of Al-alloy 2024 being friction stir welded together. From Schmidt and Hattel [35]

Fig. 8 shows isotherms on the surface of two plates of A2024 being friction stir welded together [35]. Notice the slight asymmetry in the field due to the rotating tool. A crucial part of any model of FSW is the condition (sliding, sticking or a combination) at the interface between the tool and the matrix and how it affects the heat generation. Some suggestions for this have been given in literature, among them the one by Schmidt and Hattel [33], where the state at the surface is described by a contact state variable, δ , which relates the velocity of the contact point at the matrix surface to the tool point in contact, i.e. a dimensionless slip rate defined as:

$$\delta = \frac{v_{Matrix}}{v_{Tool}} = 1 - \frac{\dot{\gamma}}{v_{Tool}} \quad \dot{\gamma} = v_{Tool} - v_{Matrix} \quad (6)$$

An overview of the different contact conditions and the corresponding values of the state variable is given below in Table I.

TABLE I
DEFINITION OF CONTACT CONDITION. FROM SCHMIDT
AND HATTEL [33]

Condition	Matrix velocity	Tool velocity	State variable
Sticking	$v_{Matrix} = v_{Tool}$	$v_{tool} = \omega r$	$\delta = 1$
Sticking /sliding	$v_{Matrix} < v_{Tool}$	$v_{tool} = \omega r$	$0 < \delta < 1$
Sliding	$v_{Matrix} = 0$	$v_{tool} = \omega r$	$\delta = 0$

Based on this state variable, an expression for the total heat generation at the surface of the shoulder and the probe can be derived assuming a linear combination of the contributions from sticking and sliding, see equation (7).

$$\begin{aligned} Q_{total} &= \delta Q_{sticking} + (1-\delta)Q_{sliding} = \\ &= \frac{2}{3} \pi \omega \left[\delta \tau_{yield} + (1-\delta) \mu p \right] \times \\ &\left[\left(R_{shoulder}^3 - R_{probe}^3 \right) (1 - \tan \alpha) + R_{probe}^3 + 3 R_{probe}^2 H \right] \end{aligned}$$

where τ_{yield} is the material shear yield stress at the welding temperature, μ is the friction coefficient, p is the uniform pressure at the contact interface, ω is the angular rotation speed and α is the cone angle. More details can be found in Schmidt and Hattel [33].

When modeling the heat generation in numerical models of FSW, different approaches can be taken. The above given expression focuses on a model where all the heat is prescribed as a surface flux. This, however, leaves the very important question: What should be done in the model with the volume occupied by the tool probe (pin)? It could be excluded from the thermal calculation making it adiabatic as seen from the matrix or one could assign some of the heat input as a volume flux in this volume. A thorough classification of the different approaches and their implications are given in Schmidt and Hattel [34]. A way of overcoming the problem with the probe volume is by using CFD models for the material flow in the matrix.

III.2. CFD Models of FSW

The basic assumption in these models is to treat the matrix material as a fluid. This calls for a suitable constitutive model from which the viscosity can be expressed. In literature, it is the most common for FSW to use the inverse hyperbolic sine law for the yield stress as a function of shear rate. This expression captures both the power law regime for low strain rates and the power law breakdown at higher strain rates. CFD models are typically formulated in a Eulerian frame, so that the tool is stationary, hence only rotating and the welding speed is accounted for by having incoming and outgoing material flow at the boundaries.

In Figs.9 and 10 a comparison between experiment, analytically based streamlines and such a CFD model is shown. The experiment contained of welding through a line of Cu marker material (MM) in two plates of 2024 and then unscrewing the tool as its center was aligned with the line of MM.

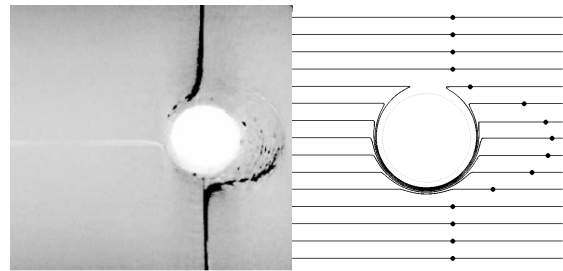


Fig. 9. Left: CT picture of weld with transverse MM. Exit hole aligned with the MM plane. Right: Analytically obtained stream lines/tracer particles. From Schmidt, Dickerson and Hattel [39]

Based on experimental findings in terms of CT pictures and comparisons with theoretical predictions by both analytical and numerical flow models, Schmidt and

Hattel [39] have proposed three characteristic zones for the flow around the tool probe: i) the rotation zone. ii) the transition zone and iii) the deflection zone, see Fig. 11.

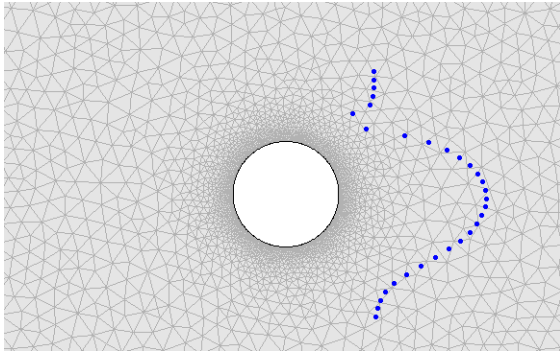


Fig. 10. Right: CFD model with simulated tracer particles. $m=0.17$. From Schmidt, Dickerson and Hattel [39]

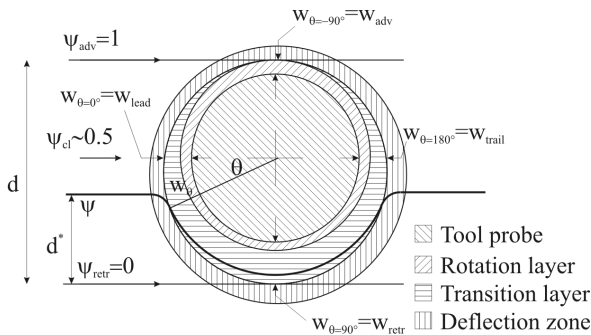


Fig. 11. Characteristic flow zones around the tool probe in FSW. From Schmidt, Dickerson and Hattel [39]

It should be mentioned that this classification is based on a simplified representation of the real, more complex flow – thus not taking into account 3D flow effects, non-symmetrical tool features (e.g. threads) and cyclic contact condition (collapse of the shear layer).

The CFD models are very suitable for analyzing the material flow during FSW, however they have some important limitations that should be mentioned: i) The residual stresses after welding which are of great importance cannot be captured, since a CFD model in nature is rate dependent only. ii) The elastic stress state in the area “far away” from the tool is not properly described. iii) The contact condition at the tool/interface is typically not very well described in the present CFD models of FSW, i.e. an a priori prescribed velocity emulating either sticking or sticking/sliding is normally used. These three limitations mentioned for the CFD models are all more or less eliminated if the material flow is described by computational solid mechanics models.

III.3. CSM Models of FSW

Relatively few solid mechanics based models of FSW have been given in literature. These models in turn

encounter obvious problems with the very large strains leading to a need for constant remeshing. Alternatively, one can use an ALE (Arbitrary Lagrangian Eulerian) approach which to some extent has the remeshing already inherently built-in to the formulation. Either way, one will face very time consuming calculations if formulated in an implicit framework. So, if the analysis is to be carried out on a normal computer, explicit models often seem to be the only solution. Of course they also have drawbacks in terms of a very restrictive stability criterion for the time step given by the CFL-number, however, this can to some extent be accounted for by the use of mass scaling.

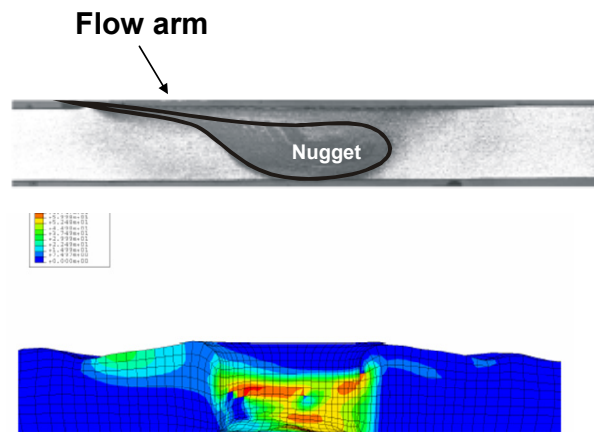


Fig. 12. Upper: Microstructure showing the well-known “flow arm” from the nugget. Lower: Numerically predicted equivalent plastic strain (in the range of 0-75) showing a similar result. From Schmidt and Hattel [6]

A comprehensive CSM model for FSW was suggested by Schmidt and Hattel [6], figure 12. The model is based on an ALE formulation in an explicit framework (ABAQUS explicit). A special feature about the model is that the heat generation between the tool and the matrix is not prescribed but part of the solution itself. This adds to the generality of the model but also to the complexity and hence the need for computational power. The model has been used to predict void formation behind the tool, being the first model in literature able to predict this.

III.4. Integrated Models of FSW

Recently, some integrated models of FSW have started to emerge in literature. Here, the author’s and co-workers’ own model, coupling CSM-based residual stress analysis with in-service load modeling is briefly presented. The considered case is the friction stir welding of a stringer to a plate and both the analysis of the residual stresses and the coupling to the subsequent load situation was carried out in ABAQUS Standard, Tutum et al. [46], see Fig. 13.

The integrated residual stress and load analysis consisted of four steps which are shown in Fig. 14.

The residual stresses along the dotted line shown in

figure 14 after welding and releasing as well as after applying the load are presented in Fig. 15.

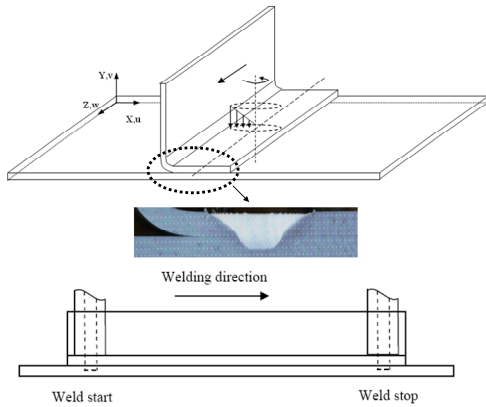


Fig. 13. Geometry of a stringer friction stir welded to a plate. Used for coupling of residual stress and in-service load analyses, from Tutum et al. [46]

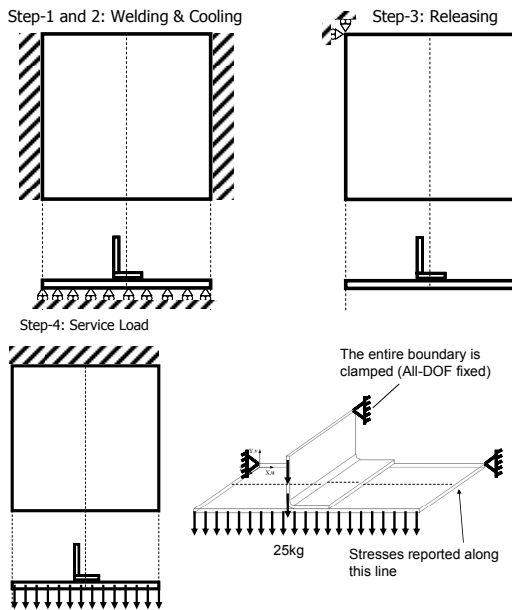


Fig. 14. The 4 steps in the coupled residual stress and in-service load analyses, from Tutum et al. [46]

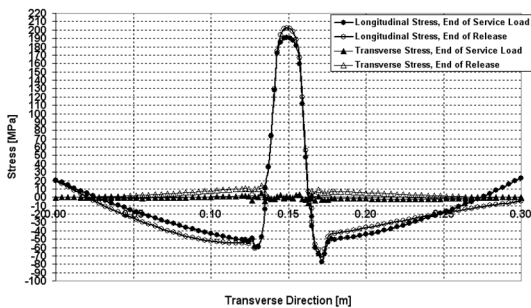


Fig. 15. Longitudinal and transverse residual stresses after welding and releasing as well as after applying the load, from Tutum et al. [46]

As seen on the figure, applying the load actually slightly reduces the longitudinal stresses in the middle of the weld. This is of course not a general statement but

only valid for this geometry and load case. Moreover, it should be emphasized, that this type of analysis obviously would benefit a lot from a prediction of the transient evolution of the mechanical properties in the structure close to the weld.

IV. Failure Analysis of a Stellite Weld on a P91 Valve

In this section the following failure case is analysed by integrated modelling: A maintenance inspection of a high pressure regulating valve in the turbine section of the Danish power plant "Skaerbaek 3" after 25.000 hours of operation at 580°C exposed a critical and total breakdown of a Stellite 6 (1.5C-30Cr-4.5W, bal Co) overlay weld (to increase wear resistance of the valve) on a steel P91 (0.1C-9Cr-1Mo-V-Nb-N) base material, see Figs. 16 and 17. A crack had grown at the fusion line between the two materials and the entire layer of coated Stellite 6 material could be removed with light tools, see Fig. 17. The Stellite 6 material was oxidized at almost the entire surface, which indicated that the crack had been open for some time. It was not possible from the oxide layer to evaluate the direction of the crack propagation since the thickness of the oxide layer did not show any systematic variation. The breakdown is of course critical since the power plant unit must be stopped during repair and the number of similar units makes it critical to get a good damage assessment to understand the nature of the breakdown. In this part of the damage assessment, focus is put on the manufacturing stages, i.e. the initial welding of Stellite onto the P91 material, the machining of the top layer weld-material and the subsequent heat treatment of the entire valve as well as on the exposure of the valve to high temperature environment during service.

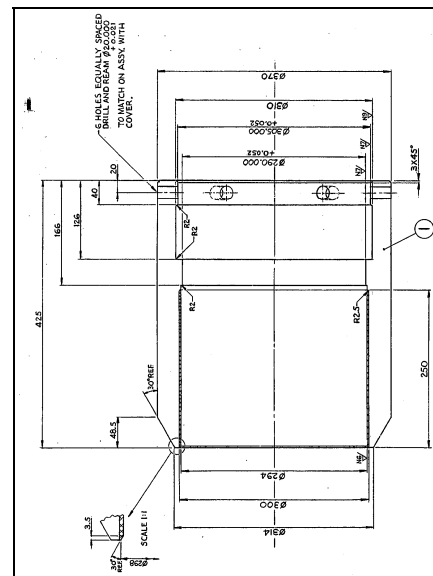


Fig. 16. HP valve of P91 with stellite layer welded on interior of cylinder

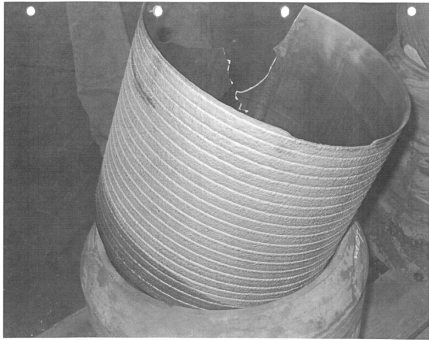


Fig. 17. Broken stellite layer in P91 valve

In order to analyse the influence of this entire chain of processes and service, an in-house FEM code has been used to model the thermomechanical history of the material. To get useful results from the numerical analysis it is imperative to couple the results from the different process stages in order to accumulate the full load history of the material. Therefore, the residual conditions from the welding and machining process are used as initial conditions for the subsequent heat treatment analysis. Finally, the residual conditions from this calculation are then used for the calculation of the in-service behaviour. In addition to these thermomechanical analyses, metallurgical effects which could reduce the strength or ductility of the Stellite 6 P91 interface are taken into account by investigating the carbon transport across the interface by multicomponent diffusion during heat treatment and in-service. This was done with the commercial software package DICTRA [47] and the resulting carbon profiles were compared with microstructures and used for the assessment of the strength development of the interface over time. The coupling of the process chain and the in-service in the numerical analysis can be illustrated by the flow chart in Fig. 18.

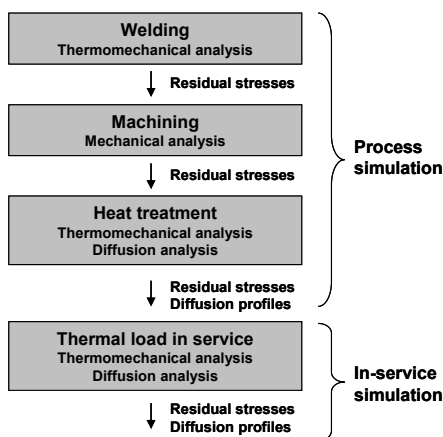


Fig. 18. Modelling of the manufacturing stages as well as the in-service conditions for the P91 steel valve

The stress history is a function of the complex thermal and elasto-plastic-viscoplastic conditions during the entire chain of calculations, see Thorborg et al. [15] for a

more thorough description. In Fig. 19, the response in the circumferential stress component $\sigma_{\theta\theta}$ during welding is governed by the heating of the P91 material giving high compression in this part of the material when the torch passes. Due to this expansion in the base material and the thermal contraction of the weld material, the circumferential stress in the weld material will be tensile at a level very much governed by the temperature dependent yield stress which increases as the weld material cools down. In Fig. 20 the profile of $\sigma_{\theta\theta}$ is shown at four points in time during heat treatment.

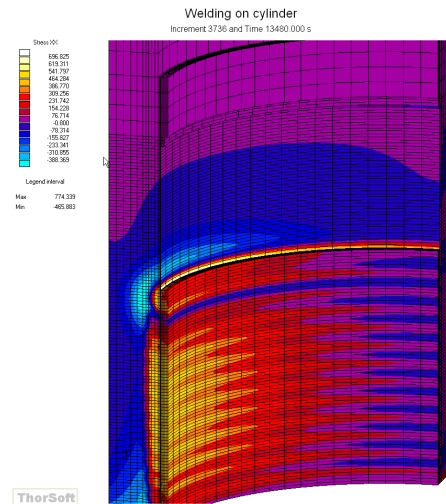


Fig. 19. σ_{xx} stress component 20s after a new weld material ring is added. At the cross section to the left, σ_{xx} will correspond to $\sigma_{\theta\theta}$ and to the right σ_{rr}

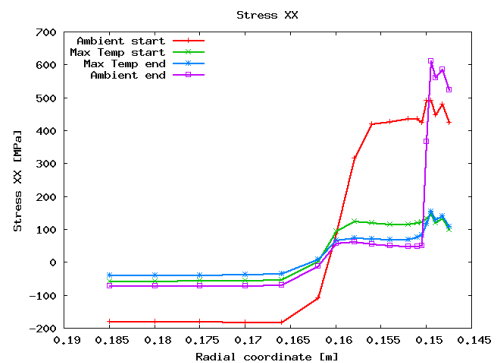


Fig. 20. Circumferential stress curve $\sigma_{\theta\theta}$ at four points in time during heat treatment. Interface at 0.15 m. Stellite to the right

It is clear that the stresses in the base material in general are reduced due to creep (shifted to the right towards the weld material) and increased in the weld material. However, across the interface, the stress gradient is quite substantial going from base to weld material. In conclusion, the heat treatment acts as stress relieving in the major part of the P91 as it is supposed to. However, very close to the weld zone, stresses in the P91

are actually increased as well as in the weld material making the overall effect of the heat treatment very questionable. The initial conditions for the wt% of C were 0,07% in P91 and 1,1% in “Stellite”. Note that Co has been substituted by Ni in the Stellite because Ni-based alloys behave similar to stellite and much more reliable data exist in the databases of DICTRA and Thermocalc for Ni as compared to for Co. In general, the calculations indicate an extremely complicated behavior at the interface, which seems to be controlled by the relative stability of the M_7C_3 and $M_{23}C_6$ carbides in the two materials. In P91 only $M_{23}C_6$ carbides are stable at the two temperatures 700°C and 580°C, whereas in the “Stellite” varying amounts of M_7C_3 and $M_{23}C_6$ carbides are stable. During post-weld heat treatment at 700°C only M_7C_3 carbides are stable and at 580°C similar mass fractions of M_7C_3 and $M_{23}C_6$ are stable in “Stellite”.

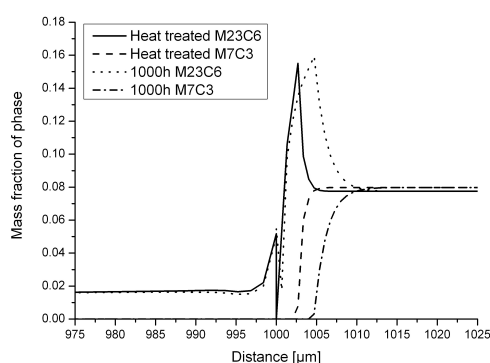


Fig. 21. Calculation of mass fractions of carbides. From start of heat treatment until 1000h in service. Interface at 1000 μm. Stellite to the right

The effect of this is that during post weld heat treatment the carbon content in the P91 steel increases, especially in the region up to ca. 3 μm from the interface, (not shown). On the “stellite” side of the interface the M_7C_3 carbides transform to $M_{23}C_6$, Fig. 21. An increased amount of $M_{23}C_6$ carbides could actually be observed in a weld between P91 and Stellite 21 after post weld heat treatment, which gives some support to this part of the calculations, Fig. 22.

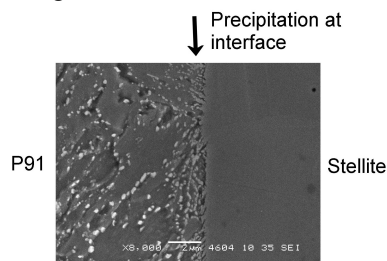


Fig. 22. Scanning electron micrograph showing precipitation at the interface between P91 and a stellite 21 (0.25C, 28 Cr, 5.5 Mo, 12 Fe, Co bal.) after 4 hours of post-weld heat treatment at 700°C. Etched in Vilella’s reagent

During service exposure at 580°C the carbon content in P91 decreases continuously. On the “stellite” side of

the interface a very narrow zone (app. 1μm) of $M_{23}C_6$ carbides forms initially fed by carbon from both the P91 and from the solution of M_7C_3 carbides in the “stellite” itself. After prolonged service exposure a zone of M_7C_3 carbides forms in the “stellite” on the backside of the narrow $M_{23}C_6$ zone, and this M_7C_3 carbide zone grows mainly by strongly accelerated carbon depletion from the P91 steel [48]. After 6400h in service a zone of app. 250μm near the interface has been severely decarburized and in particular the P91 is predicted to become completely decarburised in a 10μm wide zone near the interface, see Fig. 23.

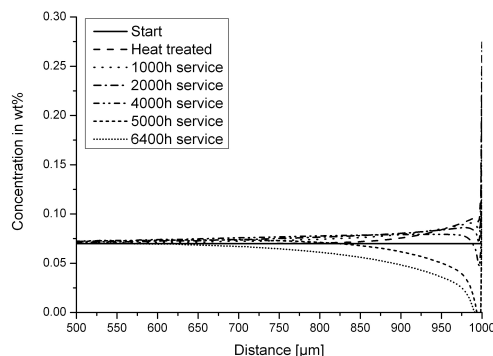


Fig. 23. Calculation of carbon profiles in P91 from start of heat treatment until 6400h in service. Corresponds to 0.15 to 0.155 m on Fig. 24

A first assessment of the effect of this decarburization on the resulting strength can now be made under the assumptions that the completely decarburised P91 has an UTS corresponding to a ferritic steel, i.e. a UTS of 300MPa at 20°C and 150MPa at 500°C. Using these assumptions, it is seen from Fig. 23 that the strength of the P91 in the zone 10 μm from the interface will reduce down to below 150 MPa after prolonged service exposure. When cooling down after service some of the strength will be regained, up to appr. 300MPa at 20°C. Comparing these findings with the residual stresses after service (before and after closing down), see Fig. 24, could very well explain the observed failure, Fig. 17, which indicated that the failure of the material had taken place at the P91 material very close to or at the very interface.

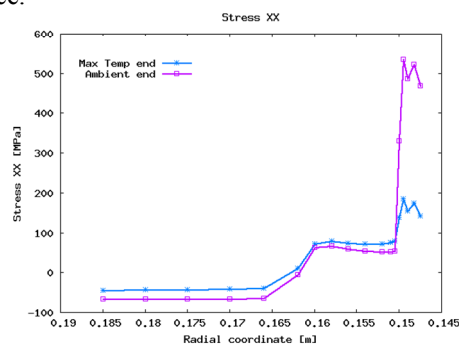


Fig. 24. Circumferential stress curve $\sigma_{\theta\theta}$ before and after cooling down at the end of service. Interface at 0.15 m. Stellite to the right

In this context it should be mentioned that the assumptions in the present calculations (Co substituted by Ni) in general do not allow a reliable estimate of the *time* to reach the decarburised level. However, based on the thermodynamics and the kinetics it is estimated that the substituting of the Co by Ni makes the process happen faster. This should be compared with the failure which took place after around 20000 h of service.

V. Conclusion

In the present paper, the focus has been on presenting three different examples of describing and analysing manufacturing processes from a holistic viewpoint of modelling materials and processes together rather than focusing entirely on isolated local phenomena taking place during the different processes. The three examples are: i) Integrated multiphysics modelling of spray forming ii) Intergated multiphysics modelling of friction stir welding and iii) Failure analysis of a premature rupture of a stellite weld on P91 valve with integrated multiphysics modelling. For all three examples, the emphasis has been put on modelling results rather than describing the models in detail and comparison and discussion with respect to experimental work and empirical observations have been given for all examples.

It is the author's firm believe that the future will bring much more examples in literature of integrated modelling of materials and processes. Moreover, it is without doubt that these kinds of models, having the possibility of optimizing entire process chains and service states, will be used much more for industrial design applications and overall optimisation in the years to come.

References

- [1] Dilthey U, Dikshev I, Mokrov O and Pavlyk V, "Software package SIMWELD for simulation of gas-metal-arc-welding processes of steels and aluminium alloys", *Mathematical Modelling of Weld Phenomena 7*, (Ed. Cerjak H et al.), 1057-1080 (2005)
- [2] http://www.esi-group.com/SimulationSoftware/Welding_heat_treatment (SYSWELD software)
- [3] Bhadeshia HKDH, "Reliability of weld microstructure and property calculations – The AWS 2004 Adams lecture explores modelling vs. experimentation for developing welding consumables for new alloys", *Welding Journal* 83 (9) 237S-243S (2004)
- [4] Zhang W, Elmer JW and Debroy T, "Integrated Modelling of thermal cycles, austenite formation, grain growth and decomposition in the heat affected zone of carbon steel", *Science and Technology of Welding and Joining* 10 (4), 574-582 (2005)
- [5] Long T and Reynolds P, "Parametric studies of friction stir welding by commercial fluid dynamics simulation", *Science and Technology of Welding and Joining* 11 (2) 200-208 (2006)
- [6] H Schmidt and JH Hattel, "A local model for the thermomechanical conditions in Friction Stir Welding", *Modelling and Simulation in Materials Science and Engineering* 13 (1) 77-93 (2005) (IOP-select)
- [7] Mishra S and Debroy T, "A heat-transfer and fluid-flow-based model to obtain a specific weld geometry using various combinations of welding variables", *Journal of Applied Physics* 98 (4) 044902 (2005)
- [8] Crumbach M, Goerdeler M, Gottstein G, Neumann L, Aretz H and Kopp R, "Through-process texture modeling of aluminium alloys", *Modelling and Simulation in Materials Science and Engineering* 12 (1) S1-S18 (2004)
- [9] A Bellini, J Thorborg and JH Hattel, "Thermomechanical modelling of aluminium cast parts during solution treatment", *Modelling and Simulation in Materials Science and Engineering*, 14 677-688 (2006)
- [10] Kermanpur A, Lee PD, Tin S and McLean M, Integrated model for tracking defects through full manufacturing route of aerospace discs", *Materials Science and Technology* 21 (4) 437-444 (2005)
- [11] Gandin Ch-A, Brechet Y, Rappaz M, Canova G, Ashby M and Schercliff H, "Modelling of solidification and heat treatment for the prediction of yield stress of cast alloys", *Acta Materialia* 50 901-927 (2002)
- [12] Myhr OR, Grong O, Fjaer HG, and C.D. Marioara, "Modelling of the microstructure and strength evolution in Al-Mg-Si alloys during multistage thermal processing", *Acta Materialia* 52 (17) 4997-5008 (2004)
- [13] Robin V, Bernauer G, Akgün T and Heubrandtner T, "Spotweld performance under high strain rate loading conditions", *Mathematical Modelling of Weld Phenomena 7*, (Ed. Cerjak H et al.), 419-434 (2005)
- [14] Lundbäck A, Alberg H and Henrikson P, "Simulation and validation of Tig-welding and post weld heat treatment on an Inconel 718 plate", *Mathematical Modelling of Weld Phenomena 7*, (Ed. Cerjak H et al.), 683-696 (2005)
- [15] J Thorborg, J Hald, JH Hattel, "Stellite failure on a P91 HP valve - failure investigation and modelling of residual stresses", *Welding in the World* 50 (1-2) 40-51 (2006)
- [16] Y. Zhou, Y. Wu and E. J. Lavernia, "Process modeling in spray deposition: a review", *Int. J. Non-Equilibrium Processing*, 10, (1997), 95-183
- [17] C. T. Crowe, M. Sommerfeld and Y Tsuji, *Multiphase Flows with Droplets and Particles*, CRC Press, 1997
- [18] JH Hattel, NH Pryds, J Thorborg and P Ottosen, "A quasi-stationary numerical model of atomized metal droplets – Part I : Model formulation", *Modelling and Simulation in Materials Science and Engineering*, 7 (3), 413-430 (1999)
- [19] NH Pryds, JH Hattel and J Thorborg, "A quasi-stationary numerical model of atomized metal droplets – Part II : Applications and assessment", *Modelling and Simulation in Materials Science and Engineering*, 7 (3), 431-446 (1999)
- [20] TB Pedersen, JH Hattel, NH Pryds, AS Pedersen, M Buchholz and V Uhlenwinkel, "A new integrated numerical model for spray atomization and deposition: Comparison between numerical results and experiments", *Proc. Int. Conf. On Spray Deposition and Melt Atomization, SDMA I*, June 2000, Bremen, Germany, 803-812 (2000)
- [21] JH Hattel, NH Pryds and J Thorborg, "A Numerical Investigation of the effect of Droplet Size Distribution on Gas Temperature during Spray Forming", *Scripta Materialia*, 42, 145-150, (2000)
- [22] I.A. Frigaard, *SIAM J. Appl. Math.* 57 (3) 1997 649-682
- [23] H.-K. Seok, H. C. Lee, K. H. Oh, J.-C. Lee, H.-I. Lee, and H. Y. Ra, *Metall. and Mat. Trans.* 31A 2000 1479-1488
- [24] P. C. Mathur, S. Annavarapu. D. Appelian and A. Lawley, *Mat. Sc. and Eng.* A142 1991 261-276
- [25] D. Bergmann and Udo Fritsching, *Int. J. Thermal Sc.* 43 (4) 2004 403-415
- [26] N.H. Pryds, JH Hattel, TB Pedersen and J. Thorborg, "An Integrated Numerical Model of the Spray Forming Process", *Acta Materialia*, 50 (16), 4075-4091 (2002)
- [27] JH Hattel, NH Pryds and TB Pedersen, "An integrated numerical model for the prediction of Gaussian and billet shapes", *Materials Science and Engineering A-Structural Materials Properties Microstructure and Processing* 383 (1) 184-189 (2004)
- [28] JH Hattel and NH Pryds, "A Unified Spray Forming Model for the Prediction of Billet Shape Geometry", *Acta Materialia* 52 (18) 5275-5288 (2004)

- [29] NH Pryds and JH Hattel, "Spray forming: A numerical investigation of the influence of the gas to melt ratio on the surface temperature", *International Journal of Thermal Sciences* 44 (6) 587-597 (2005)
- [30] R Gjesing, JH Hattel and U Fritsching, "Coupled Atomization and Spray Modelling within the Spray Forming Process using openFOAM", *Engineering Applications of Computational Fluid Mechanics* (In press)
- [31] M Song and R Kovacevic, *Mach. Tools Manuf.* 43, 605-615 (2003)
- [32] MZH Khandkar, JA Khan and AP Reynolds, *Sci. Technol. Weld. Joining* 8 165-174 (2003)
- [33] H Schmidt, JH Hattel and J Wert, "An Analytical model for the Heat Generation in Friction Stir Welding", *Modelling and Simulation in Materials Science and Engineering* 12 (1) 143-157 (2004)
- [34] H Schmidt and JH Hattel, "Heat source models in simulation of heat flow in friction stir welding", *International Journal of Offshore and Polar Engineering* 14 (4) 296-304 (2004)
- [35] H. Schmidt and J. Hattel, "Modelling heat flow around tool probe in friction stir welding" *Science and Technology of Welding and Joining* 10 (2) 176-186 (2005)
- [36] Colegrove P and Shercliff H.R.: "3-D CFD modelling of flow round a threaded friction stir welding profile" *Journal of Materials Processing Technology* 2005 169 320-327.
- [37] Askari A, Silling S, London B and Mahoney M: "Modeling and Analysis of Friction Stir Welding Processes". Symposium on Friction Stir Welding and Processing, Indianapolis, Indiana, USA, TMS, 2001.
- [38] Xu S and Deng X : "Two and Three-Dimensional Finite Element Models for the Friction Stir Welding Process". 4th International Friction Stir Welding Symposium, Park City, UT, USA, TWI, 2003.
- [39] Schmidt H, Dickerson, T and Hattel J: „Material flow in butt friction stir welds in AA2024-T3“, *Acta Materialia* 2006 (54) 1199-1209
- [40] Schmidt H. and Hattel J.: "An analytical model for prescribing the flow around the tool probe in Friction Stir Welding". Symp. on Friction Stir Welding and Processing III, San Francisco, CA, USA, TMS, 2005.
- [41] Schmidt H. and Hattel J: "CFD modelling of the shear layer around the tool probe in Friction Stir Welding". Symp. on Friction Stir Welding and Processing III, San Francisco, CA, USA, TMS, 2005.
- [42] Heurtier P., Jones M.J., Desrayaud C, Driver J.H., Montheillet F and Allehaux D.: "Mechanical and thermal modelling of Friction Stir Welding" *Journal of Materials Processing Technology* 2006 171 348-357
- [43] Schmidt H. and Hattel J.: "Modelling thermomechanical conditions at the tool/matrix interface in Friction Stir Welding". 5th International Friction Stir Welding Symposium, Metz, France, TWI, 2004.
- [44] Avilá R.E.: "A variational model for shear stress in friction stir welding based on the weld shape in transverse sections". *Modelling Simulation of Material Science and Engineering* 2006 14 689-702
- [45] Charit I. and Mishra R.S.: "High strain rate superplasticity in a commercial 2024 Al alloy via friction stir processing". *Materials and Engineering* 2003 A359 290-296
- [46] Tutum CC, Schmidt HNB and Hattel JH, *Assessment of benchmark cases for modelling of residual stresses and distortions in friction stir welding*, Proc 7th Int. Symp. On Friction Stir Welding, Japan (2008)
- [47] Borgenstam, A. Engström, L. Höglund and J. Ågren: *Journal of Phase Equilibria*, 2000, 21, 3, 269-280.
- [48] J. Hattel, J. Thorborg, K.V. Dahl and J. Hald, "Integrated Modelling of manufacturing processes and Service Conditions Analysis of Stellite Failure on a P91 HP Valve", 8th Int. Seminar *Numerical Analysis of Weldability*, Seggau, Graz, Austria, 2006

Authors' information



Jesper H. Hattel, born in Copenhagen, Denmark 1965, obtained his M.Sc. in structural engineering in 1989 and his Ph.D. in mechanical engineering in 1993 both from the Technical University of Denmark (DTU).

He currently holds a full professorship in modeling of manufacturing processes at the Department of Mechanical Engineering, DTU.

His research interests are modeling of processes like casting, joining and heat treatment in materials such as metals, polymers and concrete. Applications range from microelectronics over automotive industry to large structures like wind turbines.